INTERNATIONAL SCIENTIFIC JOURNAL OF BIRUNI
ISSN (E) 2181-2993
Volume 5, Issue 1. (2026)

INVESTIGATION OF OPTICAL AND STRUCTURAL PROPERTIES OF CDTE THIN FILMS OBTAINED BY THERMAL

K.E. Onarkulov,
A.I. Zokirov*
Fergana State University, Fergana, Uzbekistan

ABSTRACT

This study investigates the optical and structural properties of thermally evaporated cadmium telluride (CdTe) thin films with emphasis on quantum confinement effects associated with nanoscale grains (quantum-dot-like features). CdTe is a II–VI semiconductor with a direct band gap near 1.45 eV and high absorption coefficient in the visible range, making it attractive for photovoltaic and infrared optoelectronic applications. CdTe films were deposited by thermal evaporation onto three substrate types: glass (sample No. 04), photoglass (sample No. 06), and sitall (sample No. 07). Optical spectra were measured in the 200–1200 nm range, revealing strong ultraviolet absorption attributed to high-energy interband transitions. A systematic blue shift of the absorption edge was observed for the sitall-based film, indicating an increase in the optical band gap that is consistent with quantum size effects. Band-gap energies were extracted from Tauc plots for direct transitions, yielding ~1.45 eV for the glass substrate (close to bulk CdTe) and higher values (~1.48–1.52 eV) for photoglass and sitall films. Structural characterization by SEM/EDS and AFM indicates nanoscale grains and a tellurium-rich composition, which is favorable for p-type conductivity. The dielectric response was interpreted using a Drude–Lorentz model, where the Drude term accounts for free-carrier effects that enhance infrared reflectance for photoglass and sitall substrates. The results demonstrate that substrate selection and deposition conditions can tune both the optical band gap and free-carrier response of CdTe films, enabling optimization for solar-cell absorber layers and infrared photodetector applications. Future work will focus on controlled doping and process optimization to improve uniformity and device-relevant performance.

Keywords*: CdTe thin films, Quantum confinement, Drude–Lorentz model, Optical properties, Structural properties, Thermal evaporation.*

INTRODUCTION*

Cadmium telluride (CdTe), a II-VI semiconductor with a direct bandgap of approximately 1.45 eV, exhibits high absorption coefficients (>10^4 cm^{-1}) in the visible spectrum, making it an ideal material for photovoltaic applications, particularly in single-junction solar cells [1-4]. The optoelectronic properties of thermally evaporated CdTe thin films vary widely depending on parameters such as deposition time, precursor mass, and substrate type [5-8]. Recent studies have emphasized the role of nanostructures, especially quantum dots (QDs), in inducing quantum confinement effects, which lead to size-dependent bandgap widening and improved carrier mobility.

Literature indicates that thermally evaporated CdTe films typically exhibit a polycrystalline zinc-blende structure [9,10]. Film thickness and thermal processing significantly influence crystallinity and optical constants [11,12]. For instance, Lalitha et al. (2007) demonstrated that s-d orbital interactions strongly affect absorption and reflection [13]. Babar (2016) and Alam (2021) reported bandgap values ranging from 1.45–1.52 eV for varying thicknesses, attributing variations to strain and defects [14,15]. In CdTe films incorporating QDs, electronic states are modified, resulting in a blue shift of the absorption edge and enhanced nonlinear optical properties, aligning with studies on CdTe/ZnTe QDs.

Compared to bulk CdTe, QD-embedded films show higher quantum efficiency and narrower emission spectra, beneficial for optoelectronics. Key challenges include achieving uniform QD sizes and minimizing defects, addressed here through optimized deposition parameters. This work investigates the optical and structural properties of CdTe thin films, focusing on quantum confinement and free-carrier effects.

Theory/Calculation (optional)

The optical absorption coefficient α(λ) and the direct optical band gap Eg were estimated using the Tauc approach for direct allowed transitions:

$$(\alpha h\nu)^2 = A(h\nu - E_g \quad (1)$$

where $h\nu$ is photon energy and A is a constant. Extrapolation of the linear region of $(\alpha h\nu)^2$ versus $h\nu$ to zero provides E_g.

To interpret the dielectric response and the role of free carriers and interband transitions, the complex dielectric function was modeled by a Drude–Lorentz form:

$$\varepsilon(\omega) = \varepsilon_\infty - \frac{\omega_p^2}{\omega^2 + i\gamma\omega} + \sum_j \frac{f_j \omega_{0j}^2}{\omega_{0j}^2 - \omega^2 - i\Gamma_j \omega} \quad (2)$$

where ε_∞ is the high-frequency dielectric constant, is the plasma frequency, γ is the Drude damping parameter, and the Lorentz terms $f_j, \omega_{0j}, \Gamma_j$ describe interband oscillators. Increased ω_p (carrier concentration) and reduced (γ (lower scattering/defects) can enhance infrared reflectance and modify the optical response.

Quantum confinement in nanoscale grains can increase the effective band gap, qualitatively scaling as $\Delta E_g \propto 1/R^2$, where R is an effective grain radius, consistent with blue-shift trends observed for smaller grains.

Methods

CdTe thin films were prepared via thermal evaporation in vacuum. Substrates included ordinary glass (№ 04), photoglass (№ 06), and sitall (№ 07). Optical spectra were measured in the 200–1200 nm range using UV-Vis-NIR spectroscopy. Structural analysis involved SEM/EDS for morphology and composition, and AFM for surface roughness (Ra, RMS, asymmetry parameters). Dielectric functions were modeled using the Drude-Lorentz approach, and bandgap energies were determined via Tauc plots. Quantum confinement effects were accounted for in the analysis.

Results and discussion

Optical Properties

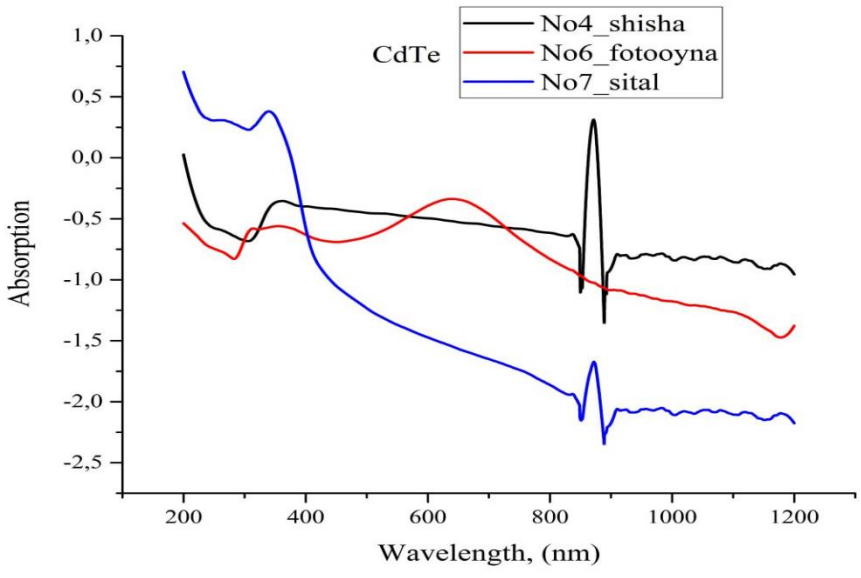

Fig. 1. Absorption spectra of CdTe thin films on glass (No. 04), photoglass (No. 06), and sitall (No. 07)

Fig.1-3 shows absorption, reflection, and transmission spectra for samples on glass (№ 04shihsa, black), photoglass (№ 06fotooyna, red), and sitall (№07sital, blue) substrates. High absorption in the UV region is attributed to high-energy interband

transitions characteristic of CdTe. In the visible range, absorption decreases gradually, forming an edge around 800–900 nm corresponding to the direct bandgap.

The absorption edge shifts blueward for the sitall substrate №07, indicating increased bandgap (Eg). This effect is weaker on photoglass and glass. Reflection spectra reveal a sharp increase in the IR for №06 and №07, linked to higher free-carrier concentration and plasma effects. Lower reflection in №04 suggests reduced carrier density.

Transmission spectra follow similar trends, with №07 exhibiting the highest values in the IR, due to superior structural order and low scattering losses.

Tauc plots ($(\alpha h\nu)^2$ vs. $h\nu$) yield Eg ≈ 1.45 eV for №04 (matching bulk CdTe), and 1.48–1.52 eV for №06 and №07, attributed to quantum confinement in nanoscale grains. The Drude-Lorentz model describes the dielectric function (2).

For CdTe films, plasma frequency ω_p increases with carrier concentration n:

$$\varepsilon(\omega) = \varepsilon_1(\omega) + i\varepsilon_2(\omega)$$

explaining enhanced IR reflection in №06 and №07. Lower damping γ in sitall samples indicates high crystallinity and low defect density.

Substrate Effects on Optical Spectra

Substrate	Key Feature	Interpretation
Glass	Stable but strong interference	Moderate quality
Photoglass	Broad, flat absorption	Optimal for PV
Sitall	High UV absorption, NIR noise	Structural, high optical noise

Drude-Lorentz fits show Lorentz dominance in 200–800 nm (interband) and Drude in >800 nm (intraband), with substrate influencing oscillator strength A and damping Γ.

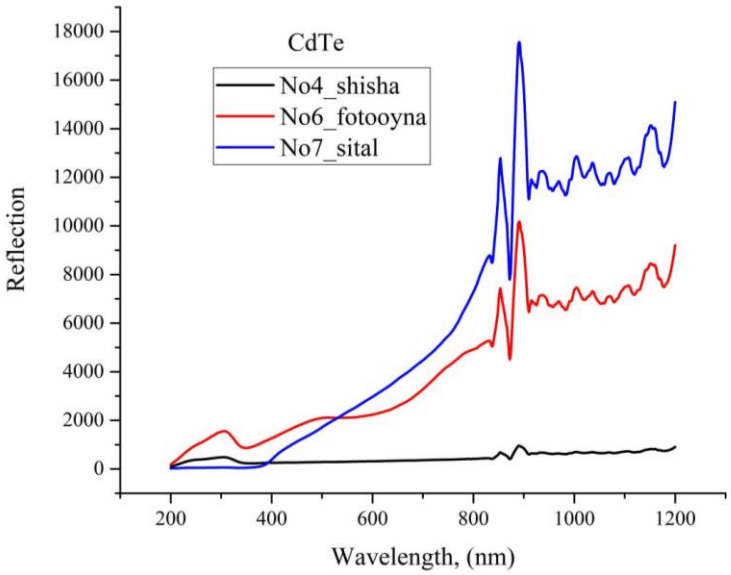

Fig. 2. Reflection spectra of CdTe thin films on glass (No. 04), photoglass (No. 06), and sitall (No. 07).

Reflection spectra (Figure 2) show lowest intensity for glass, higher for photoglass, and peaks for sitall, indicating surface modifications affect optics. Interference in photoglass and sitall suggests uniform thickness and high quality.

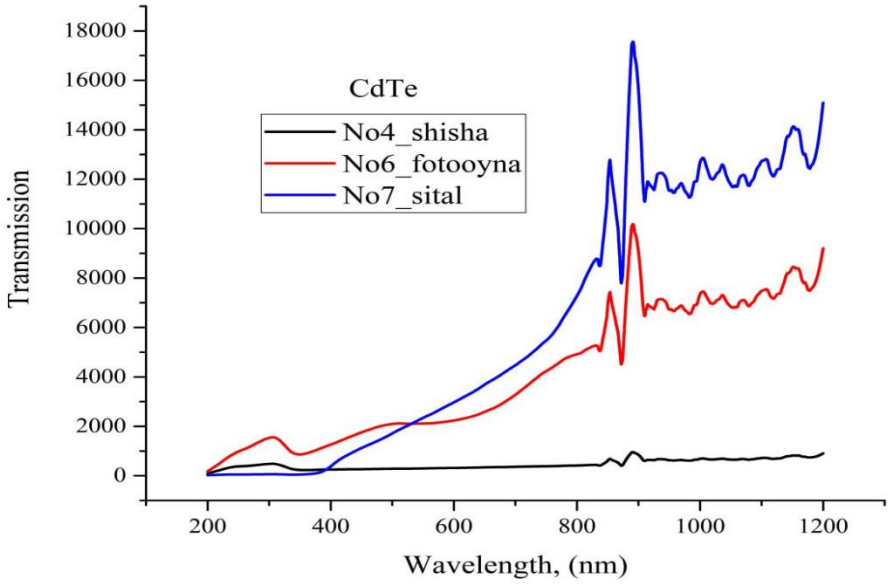

Fig. 3. Transmission spectra of CdTe thin films on glass (No. 04), photoglass (No. 06), and sitall (No. 07).

Transmission (Fig. 3) is lowest for glass, with sharp increases >800 nm aligning with $E_g \approx 1.45$ eV. Sitall yields highest transmission, confirming superior optical quality.

SEM/EDS revealed tellurium-rich composition, promoting p-type conductivity. AFM showed 2–6 nm grains, confirming QD formation. Roughness parameters indicate smoother surfaces with longer deposition, reducing defects.

Quantum confinement shifts $\Delta Eg \propto 1/R^2$, where R is grain radius, matching observed bandgap increase. This correlates with blue-shifted edges and enhanced response, consistent with CdTe QD studies.

Sitall's thermal stability enhances crystallization, boosting carrier mobility and reducing IR losses.

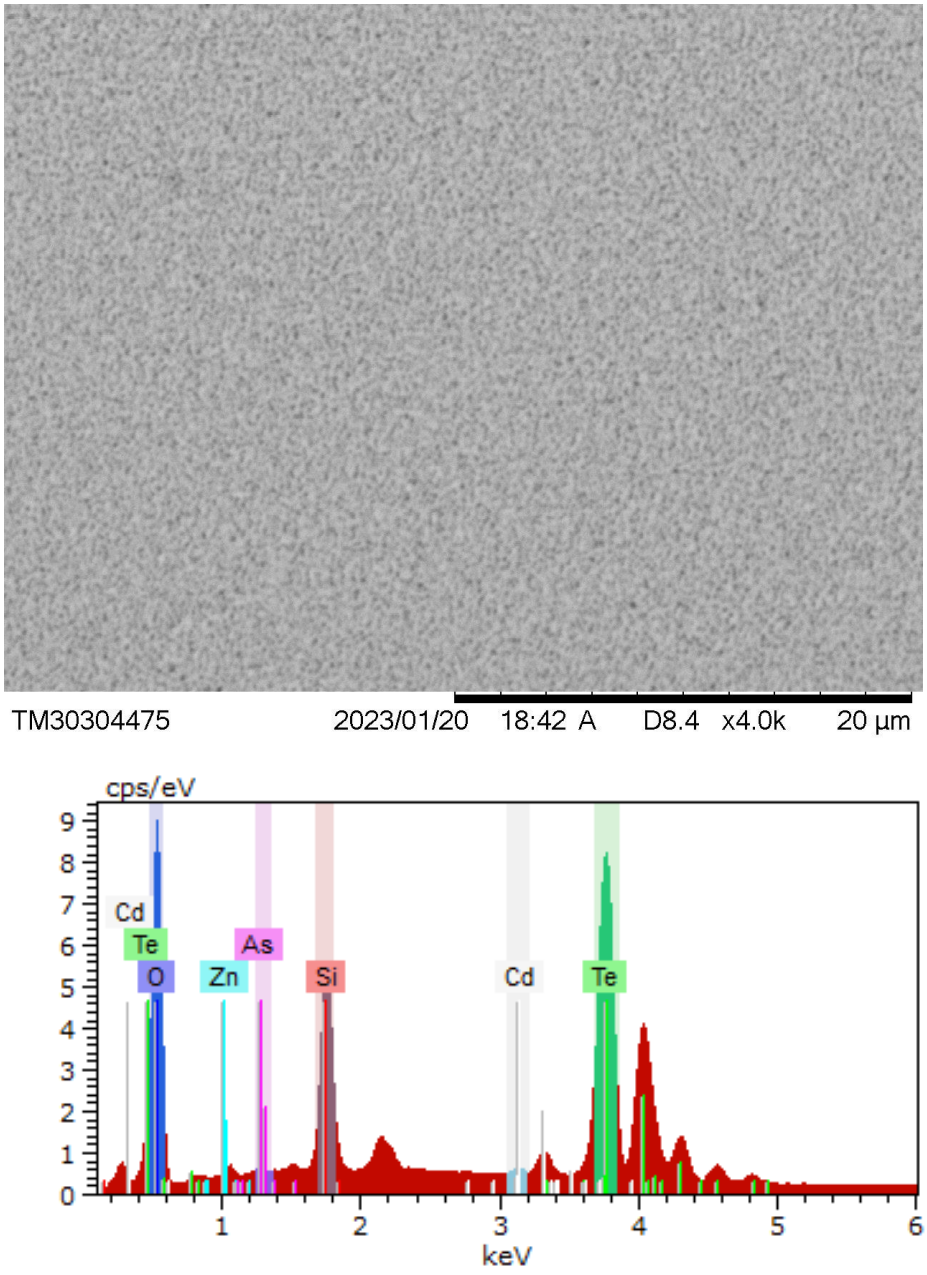

Fig. 4. SEM micrograph (surface morphology) and EDS (EDX) spectrum (elemental composition) of the CdTe thin film.

CONCLUSION

CdTe thin films prepared by thermal evaporation exhibit strong substrate-dependent optical and structural behavior. The glass-based film shows a band gap close to bulk CdTe (~1.45 eV), while photoglass and sitall substrates yield a widened optical band gap (~1.48–1.52 eV), consistent with nanoscale grain effects and quantum confinement. Enhanced infrared reflectance for photoglass and sitall films is attributed to increased free-carrier response captured by the Drude contribution in the Drude–Lorentz model. SEM/EDS and AFM results support nanoscale morphology

and a tellurium-rich composition, which may promote p-type characteristics and influence carrier-related optical effects. These findings indicate that substrate selection can be used as an effective control parameter to optimize CdTe thin films for photovoltaic absorbers and infrared photodetectors. Future work will focus on controlled doping and tighter control of grain-size uniformity to improve device-relevant performance.

REFERENCES

1. B. E. McCandless, J. R. Sites, *in:* Handbook of Photovoltaic Science and Engineering, John Wiley & Sons, 2011, pp. 600–641. https://doi.org/10.1002/9780470974704.ch14. (Wiley Online Library)
2. G. Kartopu, S. J. C. Irvine, *in:* Metalorganic Vapor Phase Epitaxy (MOVPE): Growth, Materials Properties, and Applications, John Wiley & Sons, 2019, pp. 325–353. https://doi.org/10.1002/9781119313021.ch10. (ScienceDirect)
3. D. G. Diso, Ph.D. Thesis, Sheffield Hallam University, United Kingdom (2011). (ScienceDirect)
4. A. A. Hakeem, H. M. Ali, M. M. Abd El-Raheem, et al., Optik 225 (2021) 165390. https://doi.org/10.1016/j.ijleo.2020.165390. (ScienceDirect)
5. K. Onorkulov, A. Zokirov, Bull. L.N. Gumilyov Eurasian Natl. Univ., Phys. Astron. Ser. 143 (2023) 16–23. https://doi.org/10.32523/2616-6836-2023-143-2-16-23. (bulphysast.enu.kz)
6. P. K. K. Kumarasinghe, A. Dissanayake, B. M. K. Pemasiri, et al., J. Mater. Sci.: Mater. Electron. 28 (2017) 276–283. https://doi.org/10.1007/s10854-016-5521-2. (Springer)
7. A. A. I. Lakmal, P. K. K. Kumarasinghe, V. A. Seneviratne, et al., Mater. Sci. Eng. B 273 (2021) 115406. https://doi.org/10.1016/j.mseb.2021.115406. (SSRN)
8. P. K. K. Kumarasinghe, A. Dissanayake, B. M. K. Pemasiri, et al., Mater. Sci. Semicond. Process. 58 (2017) 51–60. https://doi.org/10.1016/j.mssp.2016.11.028. (ScienceDirect)
9. V. A. Gevorgyan, N. R. Mangasaryan, V. F. Gremenok, et al., Vacuum 214 (2023) 112248. https://doi.org/10.1016/j.vacuum.2023.112248. (RSC Publishing)
10. S. Chander, M. S. Dhaka, J. Mater. Sci.: Mater. Electron. 27 (2016) 11961–11973. https://doi.org/10.1007/s10854-016-5343-2. (ResearchGate)
11. E. R. Shaaban, N. Afify, A. El-Taher, J. Alloys Compd. 482 (2009) 400–404. https://doi.org/10.1016/j.jallcom.2009.04.033. (ResearchGate)

12. S. Lalitha, R. Sathyamoorthy, S. Senthilarasu, et al., Sol. Energy Mater. Sol. Cells 82 (2004) 187–199. https://doi.org/10.1016/j.solmat.2004.01.017. (ResearchGate)
13. S. Lalitha, S. Z. Karazhanov, P. Ravindran, et al., Physica B 387 (2007) 227–238. https://doi.org/10.1016/j.physb.2006.04.008. (Wiley Online Library)
14. S. Babar, Ph.D. Thesis, University of Surrey, United Kingdom (2016). (openresearch.surrey.ac.uk)
M. A. E. Alam, Ph.D. Thesis, Sheffield Hallam University, United Kingdom (2021). https://doi.org/10.7190/shu-thesis-00452. (Semantic Scholar)